



ISSN NO. 2320-5407

Journal homepage: <http://www.journalijar.com>

INTERNATIONAL JOURNAL
OF ADVANCED RESEARCH

RESEARCH ARTICLE

Removal of heavy metal ions from aqueous solutions by radiation-induced Chitosan/(Acrylamidoglycolic Acid-co-Acrylic acid) magnetic nanopolymer

F. I. Abou El-Fadl¹ and H. L. Abd El-Mohdy*^{1,2}¹National Center for Radiation Research and Technology, P.O. Box 29, Nasr City, Cairo, Egypt²Department of Chemistry, Faculty of Arts and Sciences, Northern Border University, Rafha, Saudi Arabia**Manuscript Info****Manuscript History:**

Received: 25 October 2014

Final Accepted: 22 November 2014

Published Online: December 2014

Key words:

Hydrogel, magnetic nanopolymers, magnetic nanoparticles, heavy metals, absorption

Corresponding Author*H. L. Abd El-Mohdy****Abstract**

An effective method was developed to isolate toxic heavy metal ions from the aqueous solution by the magnetic nanopolymers. The magnetic sorbent was prepared with radiation-induced crosslinking polymerization of chitosan (CS), 2-acrylamido-glycolic acid (AMGA), and acrylic acid (AAc) which stabilized by magnetite (Fe₃O₄) as nanoparticles. The formation of magnetic nanoparticles (MNPs) into the hydrogel networks was confirmed by fourier transform infrared (FTIR) spectroscopy, X-ray diffraction (XRD), transmission electron microscopy (TEM) and Scanning electron microscopy (SEM) which revealed the formation of MNPs throughout the hydrogel networks. The swelling behavior of the hydrogels and magnetic ones was evaluated at different pH values. The adsorption activity for heavy metals such as Cu²⁺ and Co²⁺ by non-magnetic and magnetic hydrogels, Fe₃O₄/CS/(AMGA-co-AAc), in terms of adsorption amount was studied. It was revealed that hydrogel networks with magnetic properties can effectively be utilized in the removal of heavy metal ions pollutants and provide advantageous over conventional ones.

Copy Right, IJAR, 2014.. All rights reserved.

Introduction

Heavy metal ion pollution is a major environmental problem due to their high toxicity, carcinogenicity and rapid global industrialization [1–3]. Furthermore ions of toxic heavy metals such as Cu, Co, Cr, Cd, Zn, and Zr are resistant to biological degradation and can accumulate in humans, causing health issues [4–6]. Also, nickel, cobalt and copper are such metals, which are frequently present in polluted water from various industrial processes, such as catalysts, mineral processing, electrical apparatus, painting and coating and agricultural materials [7–9]. On the other hand, these metals are becoming scarce with their wide applications in many industrial fields resulting in the continuous increase in their price. Therefore, it is urgent to develop some new technologies to recycle these metals in the process of the wastewater treatment due to their great economic value [10]. The conventional purification processes including chemical precipitation [11], ion-exchange solvent extraction [12], electrode depositions [13], and activated carbon adsorption (14) are well known but expensive.

Magnetic nanoparticles (MNPs) have been the subject of intense research for the last few years because of their potential applications in electronic, photonic, magnetic, and biomedical materials [15–17]. Magnetic separation is a promising alternative approach for the solid–liquid phase separation of various metals [18]. The extremely small size and high surface to volume ratio of MNPs result in excellent adsorption kinetics for various metal ions in aqueous solutions [19]. To further improve the adsorption capacity of MNPs, active functionalization by various active polymers is necessary to impart surface reactivity towards various metal ions. Developing recyclable or reusable materials which do not produce any secondary waste is an important goal from an industrial perspective. Much effort has been devoted to the synthesis of organic/inorganic nanocomposites in an attempt to exploit new hybrid properties derived from various components [20,21]. Because of their small size, nanoparticles offer unique properties and magnetic nanoparticles based on iron oxide composites or hybrid materials; essentially in the form of

core-shell systems are finding great interest in various fields. The study of microscopic structure of magnetic materials started around 1870 [22] and left to the production of stable colloidal iron oxide (ferromagnetic) particles by McKeehan and Elmore [23]. Magnetic nanoparticles have attracted considerable attention to the scientist; this is due to its application in various fields such as physics, medicine, biology and materials science. Particularly, superparamagnetic materials play an important role in biomedical applications including magnetic resonance imaging for clinical diagnosis, magnetic drug targeting, hyperthermia anti-cancer strategy [24-26] and enzyme immobilization [27,28]. Magnetite (Fe_3O_4) and maghemite ($\gamma\text{-Fe}_2\text{O}_3$) are the most commonly used magnetic carriers for a variety of biomedical applications [29]. Among the various types of magnetic materials, the magnetic-polymer composites represent a class of functional materials where magnetic NPs are embedded in polymer matrixes. Incorporation of MNPs into hydrogel networks results in hydrogel magnetic nanocomposites, i.e., ferrogels in which the MNPs are stabilized by cross-linked gel networks. This can result in superior interaction between the MNPs and the gel networks thereby improving their mechanical properties. If the ferrogels are constructed from MNPs of typical size of less than 20 nm they impart superparamagnetic properties [30]. Hydrogels synthesized by employing natural polymers and magnetic materials such as iron oxide (magnetite) or maghemite have been widely used in many applications owing to their proven biocompatibility as well as quick response and sensitivity to external stimuli such as an applied magnetic field [31, 32].

The scope of this work is to report the structures and properties of radiation-induced magnetic nanopolymers which utilizing chitosan, 2-acrylamido-glycolic acid and acrylic acid in the presence of magnetite. It also, prolongs the activity of prepared magnetic nanopolymers in removal of some toxic heavy metal ions from aqueous solutions.

Experimental

Chitosan from crab shells ($\geq 75\%$ deacetylated), acrylamidoglycolic acid and acrylic acid were purchased from Sigma Aldrich, USA. Iron(II) chloride tetrahydrate (99 %) ($\text{FeCl}_2 \cdot 4\text{H}_2\text{O}$) and iron(III) chloride hexahydrate (99 %) ($\text{FeCl}_3 \cdot 6\text{H}_2\text{O}$), were purchased from Merck (Mumbai, India). Cobalt (II) chloride hexahydrate ($\text{CoCl}_2 \cdot 6\text{H}_2\text{O}$ and CuSO_4 (99%) were purchased from Sigma-Aldrich). All reagents were analytical grade and used without further purification.

Method

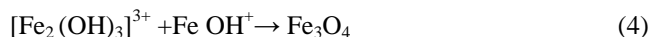
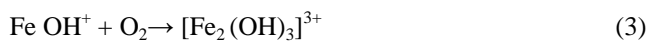
Preparation of CS/(AMGA-co-AAc) hydrogel

Firstly, different formulations of chitosan, acrylamidoglycolic acid and acrylic acid were prepared with 2% (wt/v) concentration of each polymer and monomer. After that, the mixtures were mixed by magnetic stirrer for 30 min to form homogenous polymer solutions. Finally, the solution was poured into test tubes (inner diameter 10 mm) and subjected to gamma-irradiation with a dose up to 20 kGy at ambient temperature using γ -rays from ^{60}Co source. The optimal preparation conditions, such as the compositions of chitosan, acrylamidoglycolic acid and acrylic acid, were determined later in this work. The transparent hydrogels obtained were removed, and washed with double distilled water. Table 1 describes the compositions of the prepared hydrogel formulations.

Preparation of magnetic nanopolymers

The magnetic nanopolymers were prepared by placing the previously prepared CS/(AMGA-co-AAc) hydrogel samples individually in 50 mL of double distilled water and allowed them to swell completely over a period of 24 h. Each individual hydrogel was then transferred separately to another beaker containing 200 mL of water consisting of 2.1g of $\text{FeCl}_2 \cdot 4\text{H}_2\text{O}$ and 5.8g of $\text{FeCl}_3 \cdot 6\text{H}_2\text{O}$ and allowed it for 24h to entrap the iron salts throughout the hydrogel networks. Then the polymer loaded with iron(II) and iron(III) ions were removed from the iron salt solutions, washed with double distilled water and placed in a beaker consisting of 50 mL of 0.5 M sodium hydroxide solution and left overnight. The resultant brown or black color magnetic nanopolymers were removed, washed with double distilled water, and allowed it to dry in an oven at 60°C . The properties of the final product depend on some parameters such as the ratio between Fe^{2+} and Fe^{3+} , pH and ionic strength of the medium. The following equations show the steps of formation of magnetite particles into the polymeric matrix:





Acrylamide and acrylic acid-based polymers interact with many metal cations, including hematite in hydrous solutions [33]. Due to the porous structure of hydrogels and the existence of amide (CONH_2) and carboxylic (COOH) groups in the main chains, the acrylamide and acrylic acid hydrogels easily bind to the iron (II) and iron (III) cations in aqueous mixed solutions of iron (II) chloride tetrahydrate and iron (III) chloride hexahydrate mixtures via electrostatic interactions. We therefore used such a hydrogel network as a template for the in situ deposition of magnetite iron oxide particles by utilizing the oxidation reaction induced by an ammonium solution. Fig. 1 shows the schematic illustration for the formation of this magnetite hybrid hydrogel and corresponding color changes of the swollen hydrogel during the in situ deposition process. It was found that the loading of the hydrogel with iron ions could be followed visually by the color change of the swollen polymer from white to yellow–orange (Fig. 1. a,b). The color intensity of gels depended on the iron ion concentration of the solution and was retained after washing with water, suggesting that this hydrogel bound iron ions strongly. When ammonium hydroxide was added, a rapid color change of the swollen hydrogel from yellow–orange to black was observed (Fig. 1.c). This observation indicates that the oxidation reaction takes place spontaneously and results in the formation of iron oxide particles [34].

Gel content

Dried hydrogels were extracted with distilled water for 24 h at 100°C to extract the insoluble parts of the hydrogel. The insoluble or gelled parts were taken out and washed with hot distilled water for the removal of the soluble parts and then were dried and weighed. This extraction cycle was repeated until the weight become constant. The gel yield of hydrogel was determined as follows:

$$\text{Gel (\%)} = (W_e / W_d) \times 100 \quad (5)$$

where, W_d and W_e represent the weights of the dry hydrogel and the gelled part after extraction, respectively.

Swelling studies

The dried CS/(AMGA-co-AAc) hydrogels and magnetic nanocomposite ones (1.6 mg) with different compositions were equilibrated in distilled water at 30°C and buffer solutions at different pH values (1.2, 3.5, and 5) until constant weight. The equilibrium swelling capacity (Q) of hydrogel was calculated with the following equation:

$$Q (\%) = (W_s - W_d / W_d) \times 100 \quad (6)$$

where, W_s and W_d are the weights of swollen and dry samples, respectively.

Metal uptake measurement

The fixed weight of the prepared gel was immersed in different metal ion feed solutions in the range of 2-20 mg/ml at 8 hours. Merck atomic absorption standard solutions of these metals were used for the calibration process. The effect pH of metal feed solutions on the amount of metal absorption was also studied from pH2 up to pH5. The remaining metal ions in its feed solutions were determined by using UV-VIS spectrophotometer at identical metal absorbance wavelength. The metal uptake (E) was calculated as follows:

$$E (\text{mg/g}) = [V (C_i - C_r)] / W \quad (7)$$

where, V is the volume of solution (l), W is the weight of hydrogel (g), whereas, C_i and C_r are the concentrations of metal ions in mg/l before and after adsorption, respectively.

Characterization of prepared hydrogels

FT-IR spectroscopy was performed for both CS/(AMGA-co-AAc) and magnetic nanopolymer samples using FT-IR spectrometer model Mattson 100, made by Unicam and was used over the range 400-4000 cm^{-1} . X-ray diffraction was used to identify the magnetic nanoparticles into the polymeric matrix. These measurements were carried out on a Shimadzu (Kyoto, Japan) X-ray diffractometer (XRD-6000 model) equipped with an X-ray tube (Cu target), and using a voltage of 40 kV and a current of 30 mA. The magnetic nanoparticles are characterized by an ISIS EDX (Oxford Instruments, Abingdon, UK) system attached to a JEOL (Tokyo, Japan) 5400 scanning electron microscope (SEM) with a voltage of 20 keV. This SEM was used to investigate the morphologies of different polymers at high magnification and resolution by means of an energetic electron beam. The thermal analysis of polymeric samples were carried out on a Shimadzu 30 (TGA-30) at a heating rate of 10°C/min. in air over a temperature range from room temperature to 600°C. Transmission electron microscopy (TEM) was performed with a JEOL 100CX JEM operating at 80 kV. It is used to determine the size of iron nanoparticles inside the polymeric matrix. To image the magnetic nanopolymers on the TEM, finely ground polymer samples were dispersed in 1 mL of ethanol and then they sonicated to get a solution of magnetic nanoparticles. Approximately 10–20 μL of this solution was dropped onto a 3 mm copper grid, which was then dried at room temperature. Finally, the copper grid was inserted into the transmission electron microscope. UV/VIS spectrometer model UV2 series made by Unicam, was used at a wavelength range at 190-900 nm.

Results and discussion

To act as a successful adsorbent, a material must have a large internal porosity with an adequate surface area for the adsorption process. Although nanoparticles have an enormous surface area for adsorption, poorer diffusion limits the adsorption rate and overall adsorption capacity. The combination of hydrogel networks (offering enormous diffusion) and MNPs (offering enormous surface area) is an attractive potential solution in many potential applications. Therefore, the HMNCs were developed in the present investigation by dispersing the colloidal MNPs throughout the CS/(AMGA-co-AAc) hydrogels. The use of CS in this study is due to its hydrophilicity, biocompatibility, biodegradability, and greater affinity for many bio-macromolecules. In addition, CS can efficiently contribute to the stabilization of MNPs and extraction of metals. Photographic pictures of different CS/(AMGA-co-AAc) hydrogel compositions before and after Fe-loading, (A, B and D) & (A', B' and D'), respectively are shown in Figure 2.

Fig. 1 Schematic representation of magnetite nanoparticles in hydrogel network (a) swollen hydrogel, (b) iron ions loaded hydrogel, and (c) magnetite nanoparticles in hydrogel matrix.

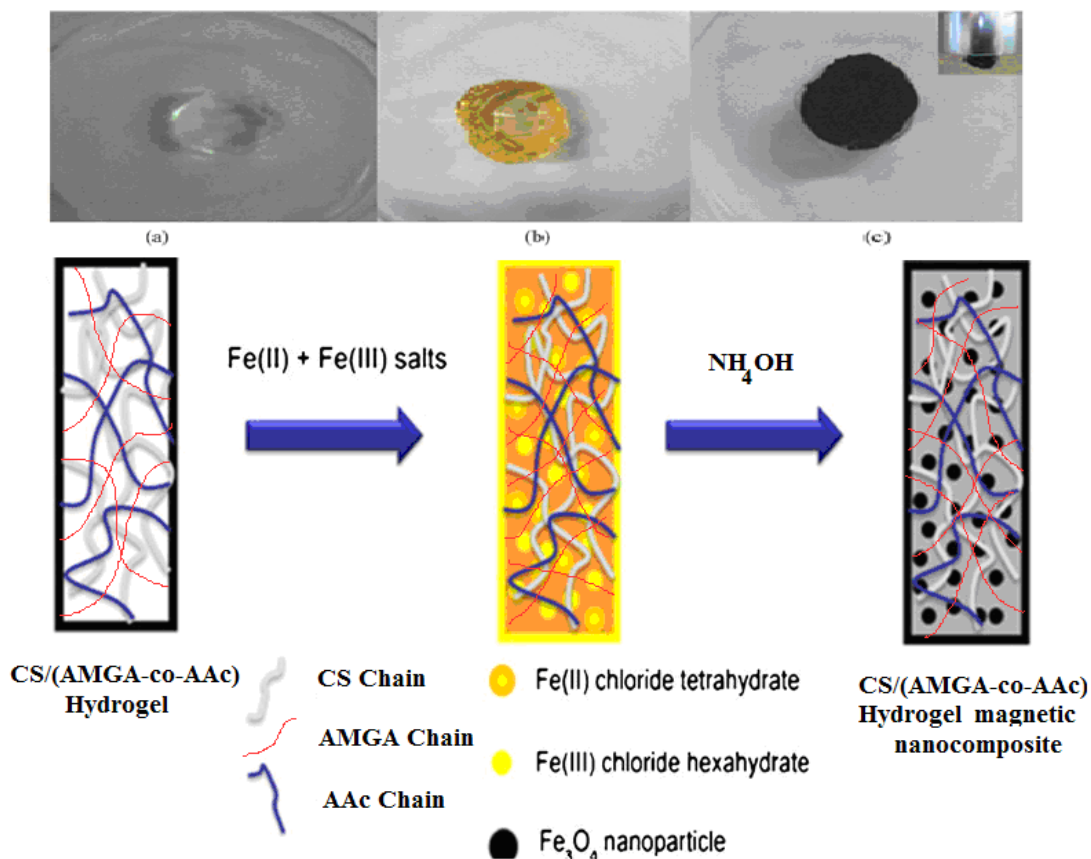
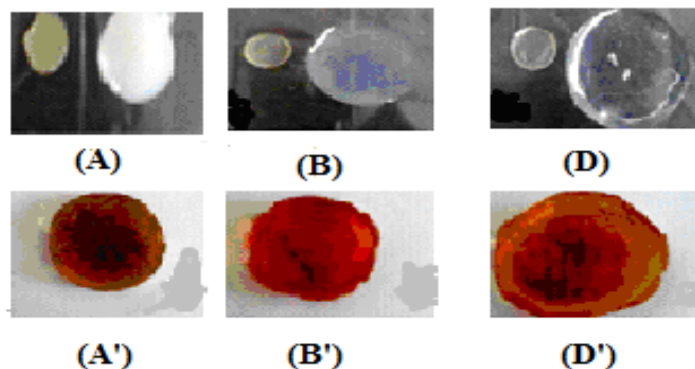


Fig. 2 Photographic pictures of different CS/(AMGA-co-AAc) hydrogel compositions before (A, B and D) and after (A', B' and D') Fe-loading.



Gel content

To evaluate the degree of crosslinking quantitatively, gel fraction of hydrogels was investigated. Table 1 shows the change in the gel content of CS/(AMGA-co-AAc) hydrogels with various CS: AMGA: AAc compositions. The gel fractions were found to have high content with increase both AMGA and AAc contents. It reduced with enhancing the natural polymer as well as chitosan content in the CS/(AMGA-co-AAc) polymeric matrix. The results cleared that the synthesized polymers (AMGA and PAAc) help in increase of the degree of crosslinking as a result of interaction among $-COOH$ and $-OH$ groups in AAc and $-OH$, $C=O$ & $-NH$ groups in AMGA matrix via hydrogen bonding [35-37].

Table 1 The gel content of CS/(AMGA-co-AAc) hydrogels with different CS: AMGA: AAc compositions (wt%).**Table 1.**

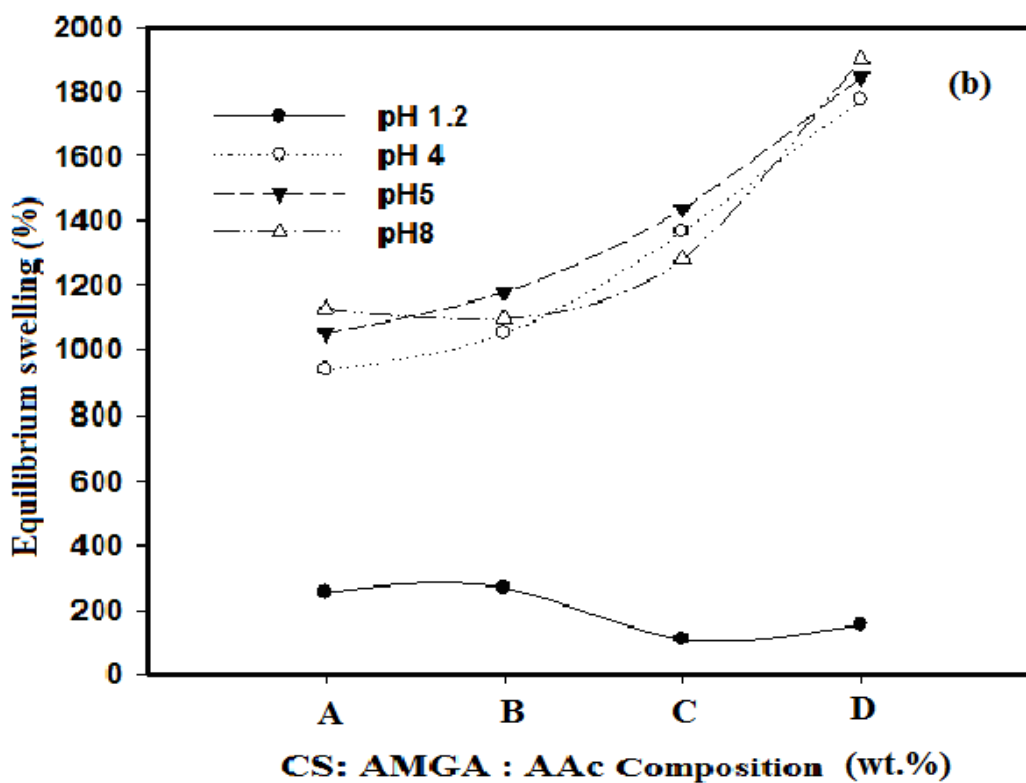
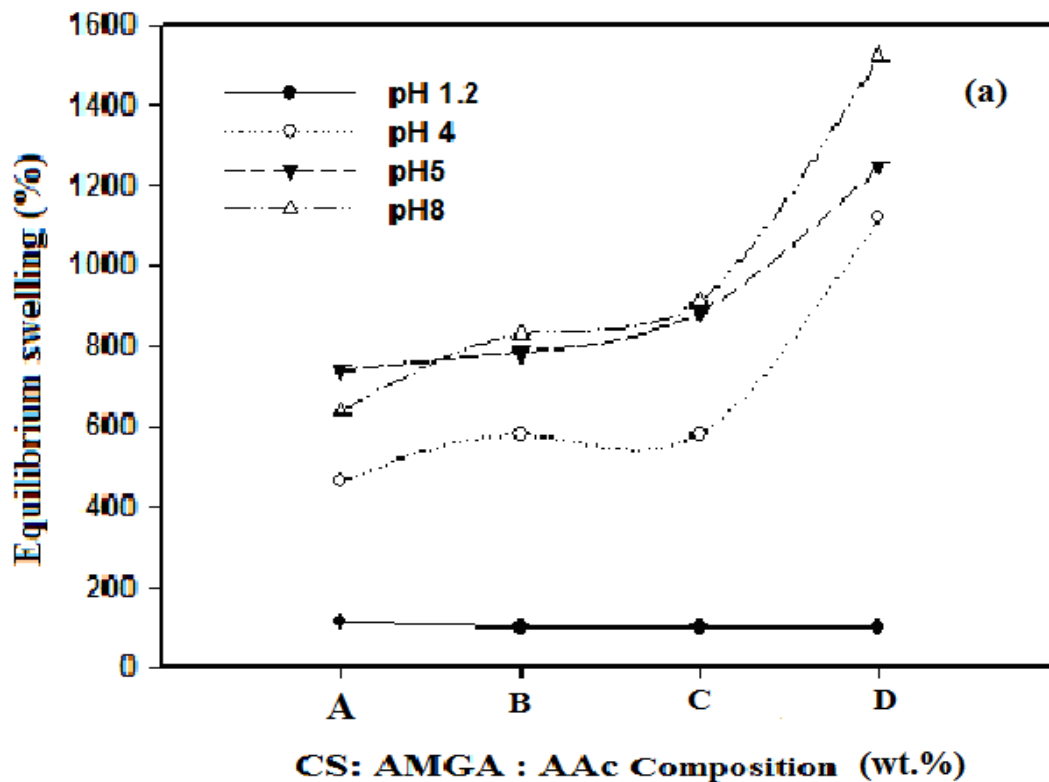
Hydrogels	CS (%)	AMGA (%)	AAc (%)	Gel (%)
A	70	20	10	85.56
B	50	30	20	91.14
C	30	40	30	92.74
D	20	40	40	93.74

Equilibrium swelling

As three-dimensional hydrophilic crosslinked polymeric networks, hydrogels are capable of swelling in distilled, drinking, ground, and sea waters or even biological fluids without dissolving or losing their structural integrity. The swollen state of hydrogels is a consequence of the balance between cohesive and dispersive forces on the hydrated polymer chains. The hydrophilic nature of hydrogel materials is due to the presence of polar and/or ionizable groups such as $-\text{OH}$, $-\text{NH}_2$, $-\text{CONH}_2$, $-\text{COOH}$, $-\text{SO}_3\text{H}$ on the polymer network [38]. These polar groups and especially the ionizable groups provide hydrogels great potential to be used as an effective absorbent for the removal of oppositely charged species especially for the elimination of toxic metal ions from contaminated waste waters.

The swelling of the CS/(AMGA-co-AAc) hydrogels was measured in deionized water and in various pH media ranging from 1.2 to 8 where the equilibrium swelling percentage of different polymer formulations are evaluated, Fig.3. Hydrogels have a great affinity to absorb water in compared with dry gels. The Figure also represents pH dependence of the equilibrium swelling percentage of CS/(AMGA-co-AAc) hydrogels (a) and magnetic ones (b) in buffer solutions from pH 1.2 to 8 where. As, the carboxylic acid units make the hydrogels pH-sensitive, the acid dissociation constant of acrylic acid is $\text{pK}_a = 4.25$. The Figure shows that, under acidic conditions (at $\text{pH} < 4.25$), anionic carboxylate groups are protonated and the network shrinks significantly, so the dissociation of carboxylic groups favors and swelling ratio of the hydrogel decreases. Also, swelling ratio increased with enhanced pH values in case of all different hydrogel compositions [39]. It also shows that the equilibrium swelling of different formulations increased for magnetic polymers in compared with nonmagnetic ones. In other words, a fast and greater affinity for water was observed for magnetic nano-polymers in comparison with the unloaded ones.

Fig. 3 Equilibrium swelling of CS/(AMGA-co-AAc) hydrogels with different CS:PAMGA:AAc compositions (a) and their magnetite ones (b) at different pH values.



FT-IR spectra

Infrared spectra of chitosan, poly acrylamido-glycolic acid and CS/(AMGA-co-AAc) hydrogels are illustrated in Figure 4. The main characteristic peaks of chitosan appeared at 3455 cm^{-1} (O–H stretch), 2879 cm^{-1} (C–H stretch), 1600 cm^{-1} (N–H bend), 1327 cm^{-1} (C–N stretch), 1155 (bridge Ostretch) and 1092 cm^{-1} (C–O stretch) are shown. The band at 2921 cm^{-1} was due to C-H stretching vibration. Also the spectrum of AMGA showed two strong bands around 1675 and 1416 cm^{-1} which correspond to the N–H bending of the NH_2 amide II band and the CN stretching of an amide III band, respectively [40]. It exhibited a common peak at 3446 cm^{-1} which is due to the NH asymmetric vibrations. The spectrum of CS/(AMGA-co-AAc) observed three new absorption peaks at 1710 and 1724 cm^{-1} correspond to the carboxyl group of grafted AAc and AMGA and peak at 1409 cm^{-1} is due to the C–O asymmetric stretching of the carboxylate anion of AAc grafted onto chitosan [41,42]. Also, there is a shift in the CN stretching of an amide III band from 1416 into 1390 cm^{-1} in addition to a broad peak appeared at 1625 cm^{-1} as a result of interaction of N–H bending of the NH_2 amide II band. The presence of a broad absorption band at 3643 cm^{-1} was due to the overlap of –OH stretching band of CS and –NH stretching band of AMGA. Accordingly, it is apparent that FTIR presented a strong evidence of graft copolymerization of both AAc and AMGA branches onto the polysaccharide backbone.

FTIR spectra of CS/(AMGA-co-AAc) magnetic polymer was presented in compared with non-magnetic one, Figure 5. The spectrum showed a shift in the CN stretching of an amide III band from 1390 into 1385 cm^{-1} in addition to a broad peak appeared at 1662 cm^{-1} as a result of interaction of N–H bending of the NH_2 amide II band. A sharp peak appearing at 583 cm^{-1} due to the stretching vibrations of the Fe–O–H confirms the presence of iron oxide nanoparticles in the polymer networks.

Fig. 4 IR spectra of CS, PAMGA and CS/(AMGA-co-AAc) hydrogel.

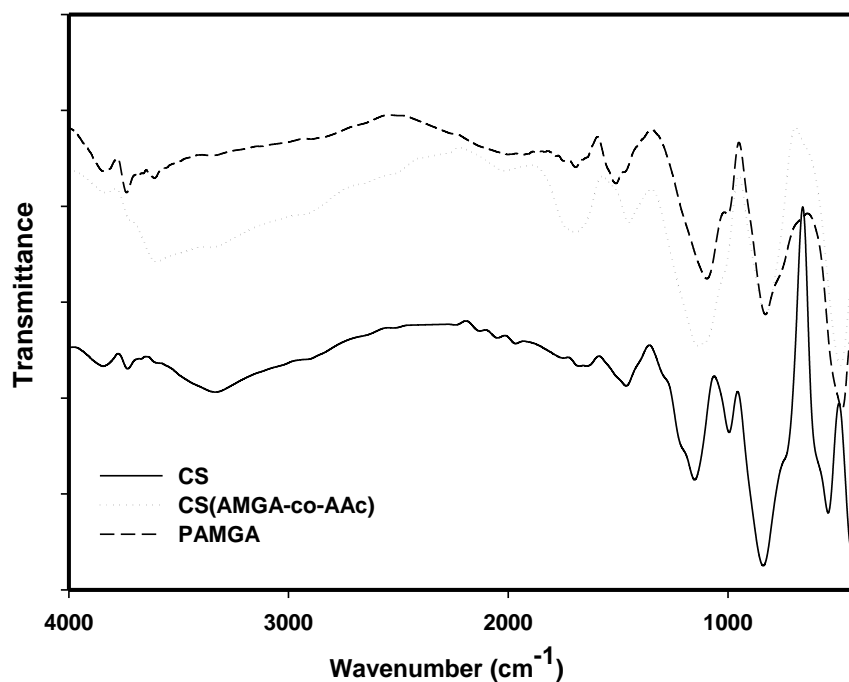
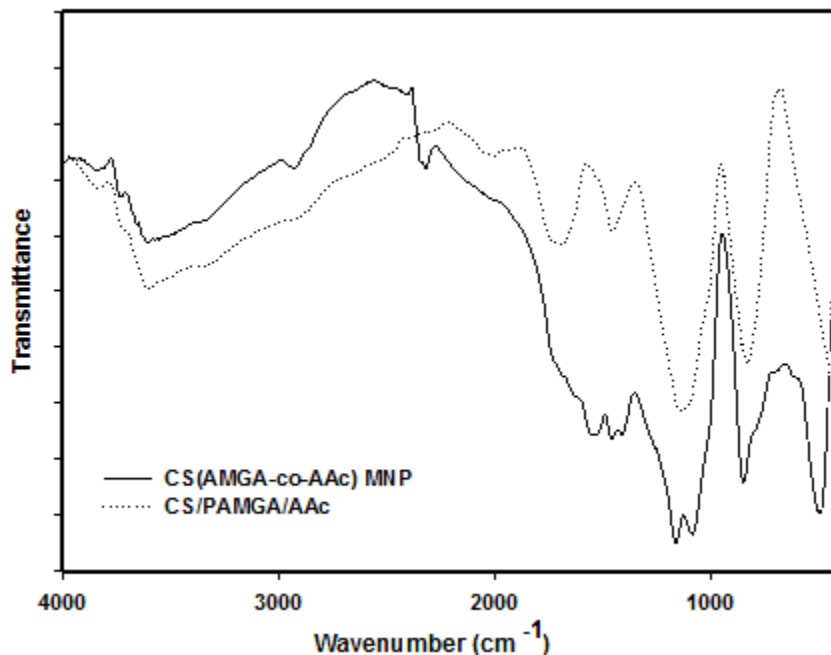


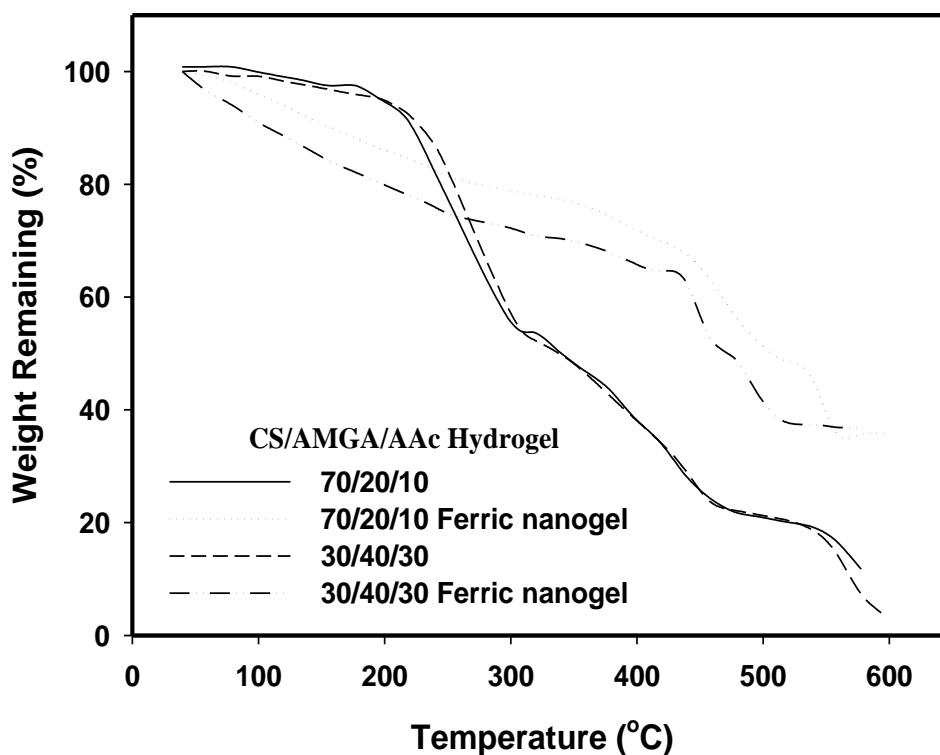
Fig. 5 FT-IR spectra of CS/(AMGA-co-AAc) and its magnetic nanocomposite hydrogel.



Thermal properties

TGA thermograms of the two different CS:AMGA:AAc hydrogel compositions reveal that there are three distinct steps of weight loss, Fig.6. It is suggested that during the initial stage of the thermal diagram, from the ambient temperature to 200 and 260 °C for both neat CS(AMGA-co-AAc) and nano magnetic gels, respectively. The weight loss is due to a dehydration process of the water contained in such hydrogels. During the second stage, from 200 to 300 °C for neat and 260 to 435 °C for nanomagnetic gels, there is decomposition in the side groups and branches of the hydrogels; magnetic hydrogels have the lowest weight loss. During the third stage, beyond 300 and 435°C for neat and nanomagnetic gels, respectively, the weight loss is due to main-chain scission in the polymer chain and matrices which result in rapid decomposition into ammonia, carbon dioxide and volatile hydrocarbons [43]. Results show that the magnetic nanocomposite hydrogels are thermally stable than the neat hydrogels.

Fig. 6 Thermal diagram curve for two different CS:AMGA:AAc compositions and their ferric nanogels at irradiation dose; 20 kGy.



Morphology of polymeric hydrogels

Morphology of the samples can be studied either by scanning electron microscopy or transmission electron microscopy studies. Figure 7 shows the surface morphology (SEM) images for both CS(AMGA-co-AAc) hydrogels (a) and magnetic hydrogels (b). A porous and rough surface was observed on the CS(AMGA-co-AAc) hydrogel morphologies and tight surface has been observed for magnetic hydrogel morphologies. The surface morphology of the neat hydrogel changed significantly after the introduction of Fe-nanoparticles. No separation phase between the neat hydrogel and the gel loaded with Fe_3O_4 nanoparticles was observed. This is indicative of the occurrence of an excellent dispersity [44]. It would be reasonable to conclude that the magnetic hydrogel is relatively dense and homogeneous.

Transmission electron microscopy provides very useful information about the size particle, polydispersity profile, and location of the magnetite nanoparticles inside and outside of the material. To probe into the morphologies and size of Fe-nanoparticles, TEM micrographs of Fe-nanoparticles are shown in Fig. 8 a,b. It is obvious that these Ag nanoparticles assume spherical-like morphologies in appearance at nanoscale levels. As it was already mentioned, Fe^{2+} or Fe^{3+} can combine with oxygen and nitrogen atom existing in the hydrogel networks via a weak coordinating bond forming O-Fe^{2+} & O-Fe^{3+} and/or N-Fe^{2+} & Fe^{3+} coordinating bonds, and thus abstracting Fe^{2+} or Fe^{3+} particles. Therefore Fe ions may uniformly be fixed and distributed in the hydrogel networks [45].

Fig. 7 SEM images for the CS/PAMGA/Ac hydrogels (a) and CS/PAMGA/Ac nanomagnetic hydrogels (b).

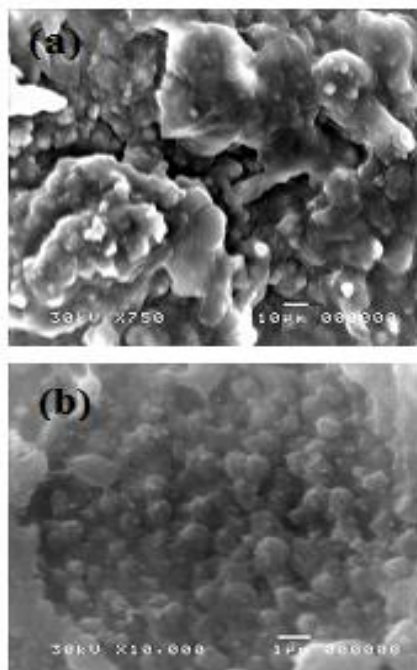
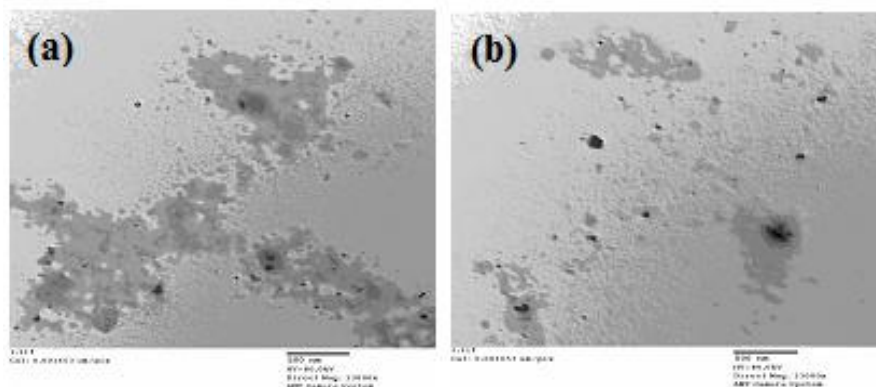


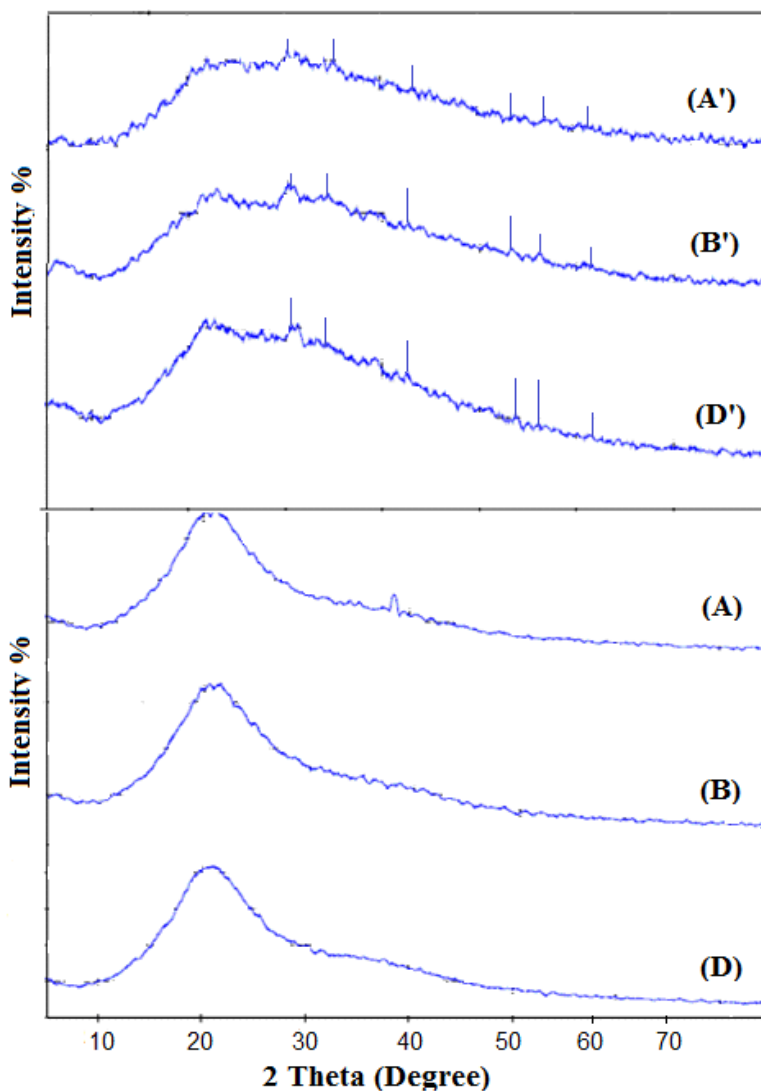
Fig. 8 TEM images for CS/PAMGA/Aac magnetic hydrogels: (a) is A composition and (b) is D composition.



Structural properties by X-ray diffraction

Fig. 9 shows the X-ray diffraction spectra for the CS(AMGA-co-AAc) hydrogel and CS/PAMGA/Aac magnetic hydrogel. In this diffractogram, a pattern of a well-crystallized magnetite phase may be verified. The hydrogels obtained without magnetic particles only revealed the crystallinity of the CS. CS(AMGA-co-AAc) magnetic hydrogel shows characteristic 2θ reflections at 30.2 (220), 35.6 (311), 43.2 (400), 53.61 (422), 38.51 (512), 57.71 (511) and 62.11 (441) that indicate the formation of a nanocrystalline spinel phase, due to the Fe_3O_4 nanoparticles entrapped into the hydrogel structure. After embedding the magnetic nanoparticles into the hydrogel structure, a change in the crystalline planes was observed, due to interaction of iron ions with polysaccharide groups, setting up a new conformation. This result can be attributed to a cubic spinel structure, revealing an efficient entrapment of magnetite at the hydrogel structure [34].

Fig. 9 XRD patterns of CS(AMGA-co-AAc) hydrogels (A, B, D) and CS(AMGA-co-AAc) magnetic ones (A', B', D').



Extraction of heavy metal ions from feed solutions

Although many technologies have been developed to purify the industrial wastewater containing heavy metal ions, their emphases are mainly focused on the extraction of metal ions from aqueous solution to avoid the environmental pollution [46–49]. For example, these metal ions are usually converted into chemical precipitation for burning or discarding. However, the resource shortage for these metals is becoming more urgent with the development of modern industry. Much attention is being drawn to develop some more efficient methods to recover metal ions currently in the process of the wastewater treatment.

Figures 10 a,b and 11 a,b, showed the absorption capacity of different compositions of the nonmagnetic and magnetic polymers for both Cu(II) and Co(II) ions in their feed solutions, respectively. The Figures observed an increase in the absorption capacity of the magnetic and nonmagnetic polymers for both Cu(II) and Co(II) ions with increase in metal ion concentration up to reach saturation, after this behavior, it may be stopped and/or decreased. The metal ion absorption was changed according to the difference in polymer compositions and magnetic properties of prepared polymers. As can be seen from figures it observed a high increase in the absorption capacity of the magnetic and nonmagnetic polymers for Cu(II) and Co(II) ions with increase in metal ion concentration up to reach saturation, after this, it stopped and/or decreased. Cu(II) and Co(II) absorption increased for different CS(AMGA-co-AAc) magnetic compositions in compared with non-magnetic ones. The Cu(II) ion absorption reach about 150-220 mg/g for magnetic CS(AMGA-co-AAc) compositions whereas, it was about 122-133 mg/g for non-magnetic ones. The results cleared that all absorption values of magnetic hydrogel compositions are higher than non-magnetic

ones for both Cu(II) and Co(II). The tendency for absorption of magnetic and non-magnetic CS(AMGA-co-AAc) composites is in the order of Cu(II) > Co(II). All these data shows that these kind materials can have great potential for cleaning of heavy metal ions from polluted waters. Some authors mentioned that these hydrogels have tendency to adsorb metal ions on their surfaces [50,51]. They mentioned that the presence of the NH₂ group besides the COOH group can increase the chelation degree of metal ions and hence the amount of adsorption.

Fig. 10 Effect of initial Cu⁺² feed solution on its amount adsorbed by CS(AMGA-co-AAc) hydrogels (a) and its magnetic nano-particles (b) with different CS:AMGA:AAc compositions. Irradiation dose; 20 kGy and treatment time; 8 hs.

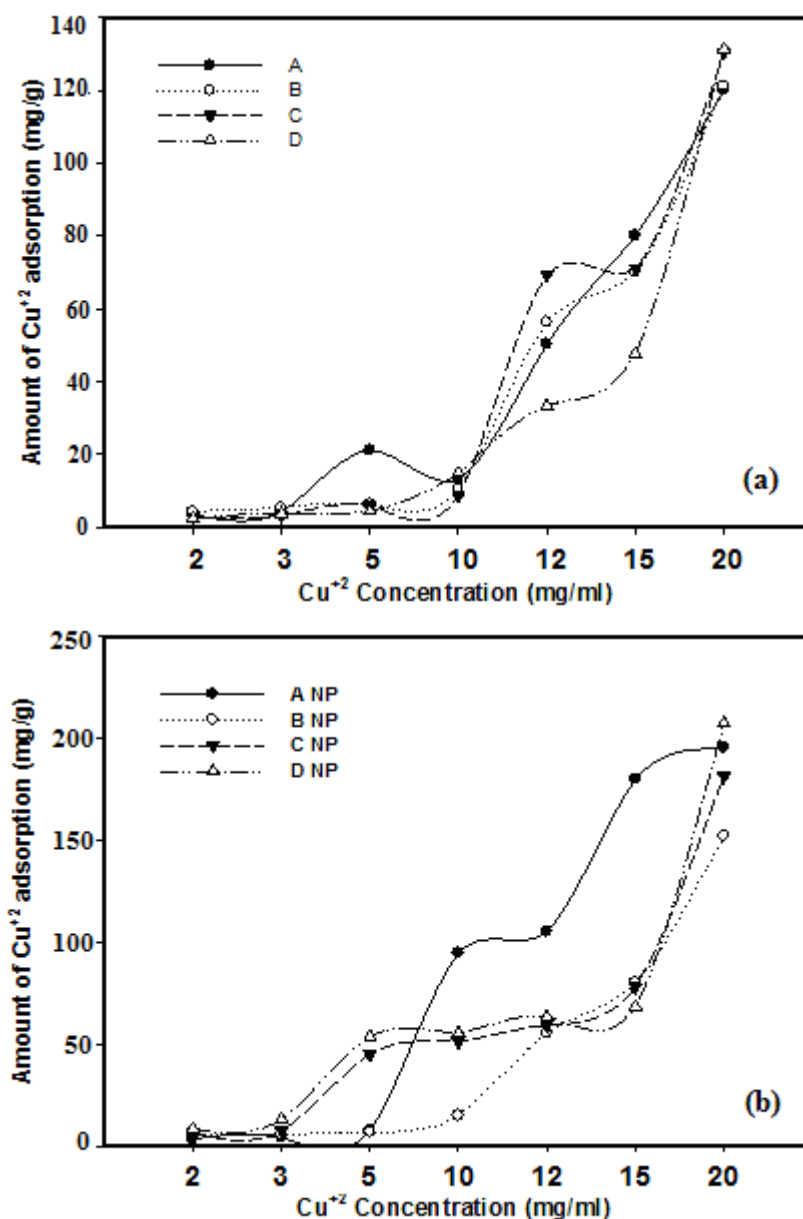
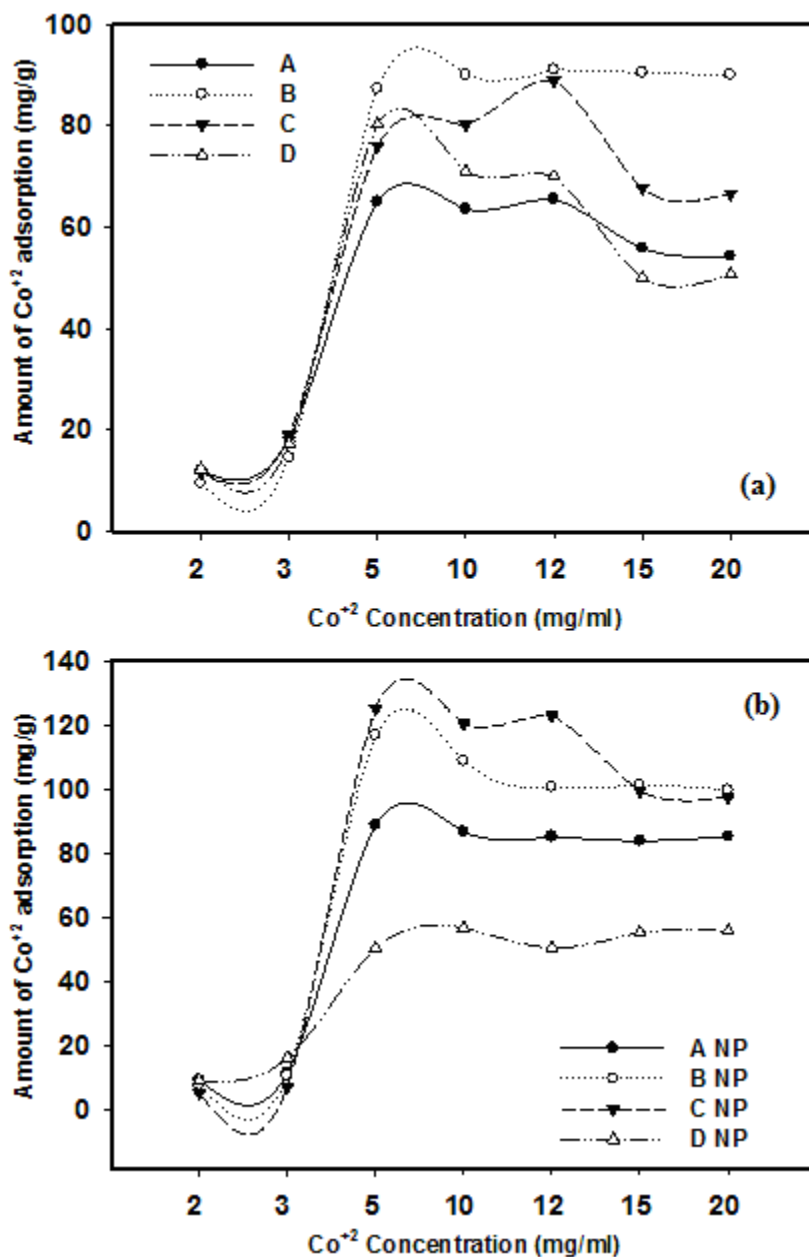


Fig. 11 Effect of initial Co⁺² feed solution on its amount adsorbed by CS(AMGA-co-AAc) hydrogels (a) and its magnetic nano-particles (b) with different CS:AMGA:AAc compositions. Irradiation dose; 20 kGy and treatment time; 8 hs.



Conclusions

Toxic heavy metal ions (Cu²⁺ and Co²⁺) from the aqueous solution were isolated by using CS(AMGA-co-AAc) magnetic polymers that prepared by ionizing radiation. The swelling behaviors were affected by changes in pH of the aqueous solution. A fast and greater affinity for water was observed for magnetic nanopolymers in comparison with non-magnetic ones. X-ray diffraction attributed to a cubic spinal structure, revealing an efficient entrapment of magnetite at the hydrogel structure. The hydrogels obtained without magnetic particles only revealed the crystallinity of the CS, whereas the magnetic hydrogel exhibited a different crystalline structure. The morphology of the CS(AMGA-co-AAc) hydrogel surface changed significantly after introducing Fe₃O₄ nanoparticles. A porous and rough surface was observed on the CS(AMGA-co-AAc) hydrogel morphologies and tight surface has been observed on the magnetic hydrogel morphologies. The metal ion absorption was changed according to the difference in polymer compositions and magnetic properties of prepared polymers. A high increase in the absorption capacity

of the magnetic and nonmagnetic polymers for Cu(II) and Co(II) ions with increase in metal ion concentration up to reach saturation, after this, it stopped and/or decreased. Cu(II) and Co(II) absorption increased for different CS(AMGA-co-AAc) magnetic compositions in compared with non-magnetic ones. The Cu(II) ion absorption reach about 150-220 mg/g for magnetic CS/PAMGA/AAc compositions whereas, it was about 122-133 mg/g for non-magnetic ones. It was revealed that hydrogel networks with magnetic properties can effectively be utilized in the removal of heavy metal ions pollutants and provide advantageous over conventional ones.

References

- [1] S.R. Smith, *Environ. Int.* 35 (2009) 142-148.
- [2] N.K. Srivastava, C.B. Majumder, *J. Hazard. Mater.* 151 (2008)1-8.
- [3] A. Santos, S. Judd, *J. Environ. Monitor.* 12 (2010) 110-115.
- [4] S.H. Jang, G.Y. Jeonga, B.G. Mina, W.S. Lyoob, S.C. Lee, *J. Hazard. Mater.*, 159 (2008) 294-299.
- [5] L. Zhou, Y. Wang, Z. Liu, Q. Haung, *J. Hazard. Mater.*, 161 (2009) 995-1002.
- [6] Y.T. Zhou, H.L. Nie, G.B. White, Z.Y. He, L.M. Zhu, *J. Colloid. Interface Sci.*, 330 (2009) 29-36.
- [7] M.A. Keane, *Colloids Surf. A.* 138 (1998) 11-19.
- [8] M. Monier, D.M. Ayad, Y. Wei, A.A. Sarhan, *J. Hazard. Mater.* 177 (2010) 962-970.
- [9] K. Swayampakula, V.M. Boddu, S.K. Nadavala, K. Abburi, *J. Hazard. Mater.* 170 (2009) 680-689.
- [10] M. Ozmen, K. Can, G. Arslan, A. Tor, Y. Cengeloglu, M. Ersoz, *Desalinat.*, 254 (2010) 162-169.
- [11] M.M. Matlock, B.S. Howerton, D.A. Atwood, *Water Res.* 36 (2002) 4757-4764.
- [12] M. Isshiki, *Vaccum* 47 (1996) 885-892.
- [13] J. Grimm, D. Bessarabov, R. Sanderson, *Desalinat.* 115 (1998) 285-293.
- [14] R. Baccar, J. Bouzid, M., Feki, F. Montiel, *J. Hazard. Mater.*, 162 (2009) 1522-1529.
- [15] C. Burda, X.B. Chen, R. Narayana, E.I. Sayed, *Chemi. Revie.* 105 (2005) 1025-1032.
- [16] B.J., Kim, J., Bang, E.T., Hawker, E.J. Krammer, *Macromol.* 39 (2006) 4108-4113.
- [17] D.H. Kim, S.H. Kim, K. Lavery, T.P. Russell, *Nano Lett.* 4 (2004) 1841-1848.
- [18] X. Liu, Q. Hu, Z. Fang, X. Zhang, B. Zhang, *Langmuir* 25 (2009) 3-10.
- [19] O. Ozay, S. Kici, Y. Baran, S. Kubilay, N. Aktas, N. Sahiner, *Desalinat.*, 260 (2010) 57-64.
- [20] Z.H. Cao, G.R. Shan, N. Sheibat-Othman, J.L. Putaux, E. Bourgeat-Lami, *J. Polym. Sci. A Polym. Chem.* 48 (2010) 593.
- [21] D. Nguyen, E. Duguet, E. Bourgeat-Lami, S. Ravaine, *Langmuir* 26 (2010) 6086-6092.
- [22] R. Arshady, In: *Microspheres Microcapsules & Liposomes*, Vol. 3, International Editorial Board. London UK, pp. 283-311, 2001.
- [23] L.W. McKeehan, W.C. Elmore, *Phys. Rev.* 46 (1934) 529-536.
- [24] A.K. Gupta, M. Gupta, *Biomate.* 26(18) (2005) 3995-4003.
- [25] G.C. Kim, Y.Y. Li, Y.F., Chu, S.X. Cheng, R.X. Zhuo, X.Z. Zhang, *Europ. Polym. J.* 44(9) (2008) 2761-2770.
- [26] J. Qu, G. Liu, Y. Wang, R. Hong, *Advanc. Powder Technol.* 21(4) (2010) 461-470.
- [27] J. Singh, P. Kalita, M.K. Singh, B.D. Malhotra, *Appl. Phys. Lett.* 98 (2011) 123702-123709.
- [28] J. Singh, M. Srivastava, J. Dutta, P.K. Dutta, *Internat. J. Biol. Macromol.* 48(1) (2011) 170-179.
- [29] H.L. Liu, S.P. Ko, J.H. Wu, M.H. Jung, J.H. Min, J.H. Lee, et al., *J. Magn. Magn. Mater* 310(2) (.2007) 815-822.
- [30] B. Li, D. Jia, Y. Zhou, Q. Hu, W. Cai, *J. Magn. Magn. Mater.* 306 (2006) 223-230.
- [31] S.R. Bhattarai, K.C.R. Bahadur, S. Aryal, M.S. Khil, H.Y. Kim, *Carbohydr. Polym.* 69 (2007) 467-474.
- [32] L.L. Lao, R.V. Ramanujan, *J. Mater. Sci. Mater. Med.* 15 (2004) 1061-1070.
- [33] A.K. Bajpai, S.K. Bajpai, *Colloids Surf. A: Physicochem Eng. Aspects* 101 (1995) 21-29.
- [34] Sivudu, K.S., Rhee, K.Y. (2009) *Colloids and Surfaces A: Physicochem Eng, Aspects*, 349,29-37.
- [35] N. Degirmenbasi, D.M. Kalyon, E. Birinci, *Colloids Surf. B. Biointerfaces*, 48(1) (2006) 4250-4258.
- [36] M.B. Wang, Y.B. Li, J.Q. Wu, F.L. Xu, Y. Zuo, J.A. Jansen, *J. Biomed. Mater. Res. A.*, 85A(2) (2008)418-424.
- [37] A.N. Krkljes, M.T. Marinovic-Cincovic, Z.M. Kacarevic-Popovic, J.M. Nedeljkovic, *Eur. Polym. J.* 43 (2007)2171-225.
- [38] H.L. Abd El-Mohdy, H.A. Abd El-Rehim, *Chem. Engineer. J.* 145 (2008) 154-159.
- [39] H.L. Abd El-Mohdy, E.A. Hegazy, H.A. Abd El-Rehim, *J. Macromol. Sci., Part A.: Pure Appl. Chem.*, 43 (2006) 1051-1059.
- [40] X. Lu, Y.M. Mi, *Macromol.* 38 (2005) 839-846.
- [41] Y. Hu, X. Jiang, Y. Ding, H. Ge, Y., Yuan, G. Yang, *Biomaterials* 23 (2002) 3139-3145.
- [42] G.R. Mahdavinia, A. Pourjavadi, H. Hosseinzadeh, M.J. Zohuriaan, *Eur. Polym. J.* 40 (2004) 1399-1407.
- [43] Abd El-Mohdy, H.L., Hegazy, E.A., El-Nesr, E.M., Abd El-Wahab, M. (2011) *J. Polym. Res.*,18,1605-1612.

- [44] A.T. Paulino, M.R. Guilherme, E.A.M.S. deAlmeid, A.G.B. Pereira, E.C. Muniz, E.B. Tambourgi, J. Magn. Mater. 321 (2009) 2636-2643.
- [45] Z.Y. Lin, Y.X. Zhang, Y.L. Chen, H. Qian, Chem. Engineer. J. 200–202 (2012) 104-112.
- [46] M. Ozmen, K. Can, G. Arslan, A. Tor, Y. Cengeloglu, M. Ersoz, Desalination, 254 (2010) 162-170.
- [47] S.S. Ahluwalia, D. Goyal, Bioresour. Technol. 98 (2007) 2243-2250.
- [48] S. Babel, T.A. Kurniawan, J. Hazard. Mater. 97 (2003) 219-227.
- [49] A.E. Lewis, Hydrometal. 104 (2010) 222-229.
- [50] L. Wei, G. Yang, R. Wang, W. Ma, J. Hazard. Mater. 164 (2009) 1159-1166.
- [51] D. Ito, K., Miura, T. Ichimura, I. Ihara, T. Watanabe, IEEE Transact. Appl. Superconduct. 14 (2) (2004) 1551-1560.